ISSN 2347 - 3983
Volume 8. No. 6, June 2020
International Journal of Emerging Trends in Engineering Research
Available Online at http://www.warse.org/IJETER/static/pdf/file/ijeter26862020.pdf
https://doi.org/10.30534/ijeter/2020/26862020

Shear yield strength, modulus of rigidity, and modulus of rupture of nodular cast iron on Magnesium Addition

Agung Setyo Darmawan*, Agus Yulianto, Masyrukan, Pramuko Ilmu Purboputro, Gigih Nugroho Jati
*Department of Mechanical Engineering, Faculty of Engineering, Universitas Muhammadiyah Surakarta, Surakarta 57102, Indonesia
* Corresponding author: Agung.Darmawan@ums.ac.id

ABSTRACT

The purpose of this study was to investigate the effect of magnesium addition on shear yield strength, rupture modulus and rigidity modulus of nodular cast iron. Magnesium addition was carried out in the form of FeSiMg alloys. Four specimens consisting of raw material, specimens with the FeSiMg alloys addition of 50 gram, 150 gram and 200 gram were then melted in furnace at temperature of 1250 ^oC. After solidification process, the nodular cast iron was composition tested to get magnesium content by using spectrometry. Further, microstructure photograph was taken to investigate the graphite and matrix phases. Finally, the torsion test was performed to obtain shear yield strength, modulus of rupture and modulus of rigidity. The torsion test results show an increase in shear yield strength, modulus of rupture and modulus of rigidity of nodular cast iron. Increased strength and stiffness of nodular cast iron with variations in the addition of FeSiMg alloy.

Key words: FeSiMg, Graphite, Modulus of Rupture, Nodular Cast iron, Strength, Torsion Test.

1. INTRODUCTION

The metal casting industry grows in line with the development of casting techniques and methods as well as various models of cast products that flood the domestic market. The cast products are widely used in daily life ranging from household furniture [1], automotive components [2]-[4], pipes [5] ,[6], pumps [7], [8] to ship propellers [9], [10].

The cast iron is an iron alloy containing more than 1.7% carbon (C) and 1-3% silicon (Si). Other elements can be added with a view to improving properties such as strength, hardness, or corrosion resistance. Commonly added elements are Copper, Chromium, Nickel, Vanadium and Molybdenum [11].

The cast iron has a liquid temperature range that is relatively lower than steel. The liquid temperature range of the cast iron is 1147 ^oC – 1390 ^oC and the liquid temperature range of the steel is 1390 ^oC – 1538 ^oC [12]. The mechanical properties of cast iron depend on the phase configuration of microstructure, namely the size, shape and distribution of the phases. One phase that has significant influence is graphite [13]. The amount, size, and shape of graphite affect the strength, ductility, and toughness of cast iron. Besides graphite, matrix also influences mechanical properties. The cast iron matrix is the same as that found in steel, namely ferrite, cementite and pearlite [14].

The cast iron is an alloy of iron and carbon as well as steel. This material is one of the most widely used engineering materials, this is due to the ease of the manufacturing process, being able to be mass-produced, and the competitive cost of the process. Although it offers many advantages, but there are some disadvantages of cast iron, namely the ductility and toughness are not as high as steel [15]. There are also some research investigated advanced materials [16]-[18].

The grey cast iron has flake graphite in the matrix of ferrite, pearlite or a mixture of ferrite and pearlite [19], [20]. Flake-shaped graphite with sharp edges will result in high stress concentrations. This high stress concentration will affect strength and hardness.

The addition of magnesium when grey cast iron in liquid conditions will cause flake graphite turn into spheroidal graphite [21], [22]. This spheroidal graphite will cause a concentration of stress that is less than the stress concentration caused by flake graphite, lamellar graphite or vermicular graphite [23]-[25]. Spheroidal graphite in cast iron occurs when there is magnesium content in cast iron of 0.02% to 0.05%. However, due to the relatively low solubility in the iron and the vapour point is only 1107 ^oC, to prevent excessive loss when mixing, magnesium is then given in the form of FeSiMg alloy. The main properties of casting nodular cast iron will be greatly influenced by many factors starting from casting time, casting temperature, and the process of mixing metal fluids with alloy materials.

Therefore, this work is aimed at investigating the effect of adding magnesium to the shear strength and stiffness of nodular cast iron.

2. MATERIALS AND METHODS

The nodular cast iron was melted using a melting furnace. The furnace was made of refractory containers that contain metal loads. The furnace was heated by heat conduction from the walls of the container. Heating fuel was in the form of coke. The temperature used to melt the nodular cast iron was 1250 ^{o}C

The mould was made of silica sand (SiO_2) by mixing additive material, namely bentonite. The pattern was inserted into the bottom frame and filled with sand (cope), then the sand was compacted by being crushed, and provided calcium carbonate above the pattern (drag) so that the mould sand does not easily stick.

The nodular cast iron in liquid conditions with 0.0296% magnesium content added with FeSiMg alloys with variations of 50 grams, 150 grams and 200 grams. The nodularization method used an open ladle system. This system was used because it has several advantages, namely simple and extensive use, however, this system also causes losses in the form of reactions that produce steam and smoke. Further, the ladle containing FeSiMg alloy is added to the molten metal and shaken with the expectation that FeSiMg alloy can be mixed evenly so that it can produce graphite in a spheroidal shape and spread evenly. Furthermore, the liquid metal from variations FeSiMg addition was poured into the sand mould.

The mould is used for the solidification process of liquid metal to solid with an adjusted shape. The mould is made of silica sand (SiO_2) by mixing additive material, namely bentonite. The pattern is inserted into the bottom frame and filled with sand, then the sand is compacted by being pressed, and provides calcium carbonate above the pattern so that the mould sand does not easily stick. After the cast iron reached room temperature, the casting results are disassembled and cleaned. Furthermore, composition test, metallographic and torsion test were conducted.

Sanding the surface of the specimen using a sanding machine with a size of a sandpaper grid of 60, 80, 100, 320, 500, 800, 1000 and 2000, respectively to produce a flat and smooth surface. During sanding, water was flowed to avoid the effects of heating on the results of the microstructure and drain of eroded metal powder. The surface polishing of the specimen was carried out with a velvet cloth with the addition of autosol as a polishing material, with the aim of getting a shiny test surface in order to get a good reflection of light during the microstructure test process. The etching is conducted by using chemicals that are acidic. Etching functions to produce photographs of microstructure. The etching solution composition used is 95% alcohol and 5% HNO_3. Total volume of etching solution was 30 ml.

Torsion test specimens are made by turning. The dimensions of the torsion test specimens according to ASTM E143 can be seen in Figure 1. Torsion tests are performed to obtain shear yield strength, modulus of rupture and modulus of rigidity of nodular cast iron. The shear yield strength is the shear stress limit before the material undergoes plastic deformation. To find the yield strength, the 0.004 radian offset method is used in the torque moment graph of the twist angle. Modulus of rupture is the maximum shear stress due to maximum torsional load when a material breaks. While the modulus of rigidity shows the size of the stiffness of a material in its elastic region. In torsion tests, the value of the modulus of rigidity is obtained through the comparison of shear stress with shear strain that occurs in the elastic region.

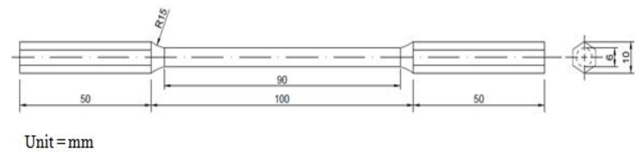

Figure 1: Dimensions of torsion test specimens

3. RESULTS AND DISCUSSIONS

Chemical composition testing aims to determine the percentage of magnesium content. This test is carried out using a chemical composition testing instrument. The results of chemical composition tests on nodular cast iron and nodular cast iron raw materials with the addition of FeSiMg can be seen in Table 1.

The test results showed that the specimen 1 (raw material) contains a magnesium composition of 0.0296%, and the test results of specimen 2 (FeSiMg alloy addition of 50 grams), specimen 3 (FeSiMg alloy addition of 150 grams), and specimen 4 (FeSiMg alloy addition of 200 grams) were 0.0307%, 0.0336%, and 0.0351%, respectively. This content reached the required magnesium content in nodular cast iron, which is between 0.02-0.08% Mg in accordance with the requirements of Atomic Fluorescence Spectrometry (AFS).

Metallographic observation of the specimen aims to determine the effect of variations in magnesium content on the nodular cast iron microstructure. This observation was carried out to determine the shape, size, and distribution of the graphite and matrix phases, and was made after the etching process so that the microstructure around graphite became clearer. Metallographic test results of the specimen can be seen in Figure 2.

The microstructure test results in Figure 2 show clearly the phases in nodular cast iron, graphite, ferrite, and pearlite. The black spheroidal graphite is seen surrounded by the brightly coloured ferrite phase in a pearlite matrix in the form of bright and dark lamellites. The phases were in accordance with the phase diagram for cast iron, which graphite will be spheroidal due to the presence of magnesium as can be seen in Figure 3 [12]. The matrix phases of cast iron were similar to the phases of steel (ferrite and pearlite) according to Figure 4 [12].

The results of the microstructure test show that the more FeSiMg alloys were added in the manufacture of cast iron the more magnesium content in the nodular cast iron. The increasing magnesium made spheroidal graphite tends to be smaller and uniform. The shape of this graphite shows that there is enough magnesium element contained in the cast iron alloy, it can be seen in the results of the microstructure test on each specimen. In addition it can also be seen that pearlite will increase and ferrite will decrease with increasing percentage of magnesium.

Variation magnesium content in cast iron from 0.0296%; 0.0307%; 0.0336% and 0.0351% can affect the value of the shear yield strength (Figure 5) and the modulus of rupture (Figure 6), as well as the shear stiffness represented by the modulus of rigidity (Figure 7). The value of the shear yield strength, the modulus of rupture and modulus of rigidity tends to increase with increasing magnesium content. This is because in the microstructure photograph, the size of the graphite and ferrite around it tends to decrease. The increasing of the shear yield strength, the modulus of rupture and modulus of rigidity also caused by the increasing pearlite. The more pearlite, the more cementite. Cementite is a compound that has ionic bonds which are stronger and harder than ferrite which has metal bonds.

Table 1: The composition test result of nodular cast iron

Element	Specimen 1 (%)	Specimen 2 (%)	Specimen 3 (%)	Specimen 4 (%)
C	3.4599	3.5100	3.5664	3.4876
Si	2.6302	2.5997	2.5926	2.6449
S	0.0147	0.0132	0.0108	0.0105
P	0.0139	0.0177	0.0152	0.0163
Mn	0.3459	0.5279	0.5034	0.5748
Mg	**0.0296**	**0.0307**	**0.0336**	**0.0351**
Ni	0.0119	0.0115	0.0114	0.0117
Cr	0.0829	0.0921	0.0889	0.0896
Mo	0.0016	0.0020	0.0017	0.0026
Cu	0.0298	0.0231	0.0213	1.1144
Ti	0.0307	0.0360	0.0349	0.0356
Sn	0.0083	0.0090	0.0887	0.0088
Al	0.0129	0.0119	0.0114	0.0130
Nb	0.0002	0.0002	0.0002	0.0011
V	0.0034	0.0045	0.0041	0.0048
Co	0.0030	0.0030	0.0029	0.0034
Ca	0.0353	0.0337	0.0322	0.0344
Zn	0.0010	0.0007	0.0005	0.0018
Fe	93.32	93.11	92.51	91.95

The lowest strength which is represented by shear yield strength and modulus of rupture and the lowest stiffness which is represented by the modulus of rigidity were produced by specimens with 0.0296% magnesium content. This specimen has the largest graphite and ferrite size, which means it has the smallest pearlite. While the highest strength and stiffness is produced by specimens with 0.0351% magnesium content. This specimen has the smallest graphite and ferrite

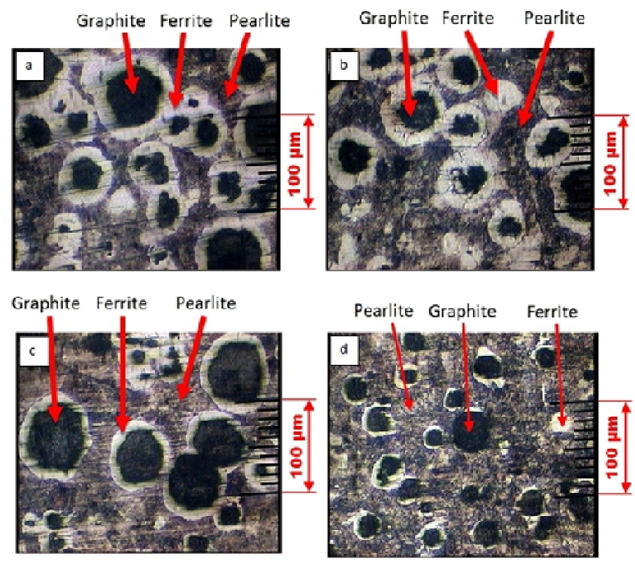

Figure 2: Microstructure of nodular cast iron (a) 0.0296% magnesium (b) 0.0307% magnesium (c) 0.0336% magnesium (d) 0.0351% magnesium

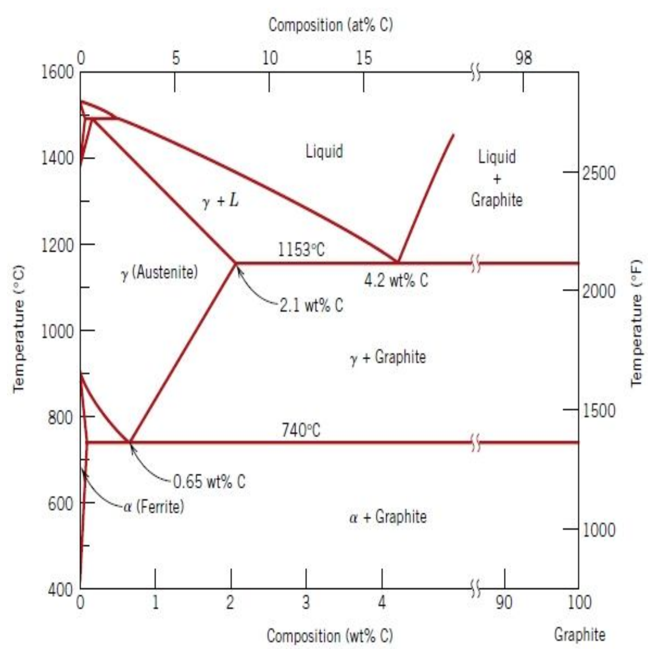

Figure 3: The equilibrium iron–carbon phase diagram with graphite, the presence of magnesium makes the shape of graphite become speroidal

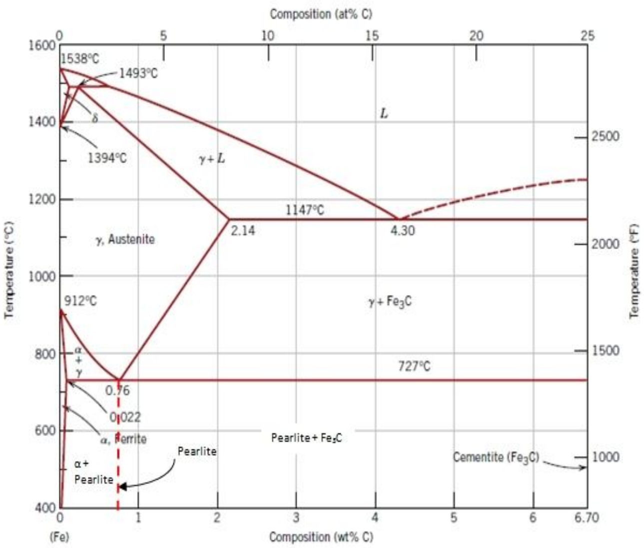

Figure 4: The equilibrium iron–carbon phase diagram without graphite

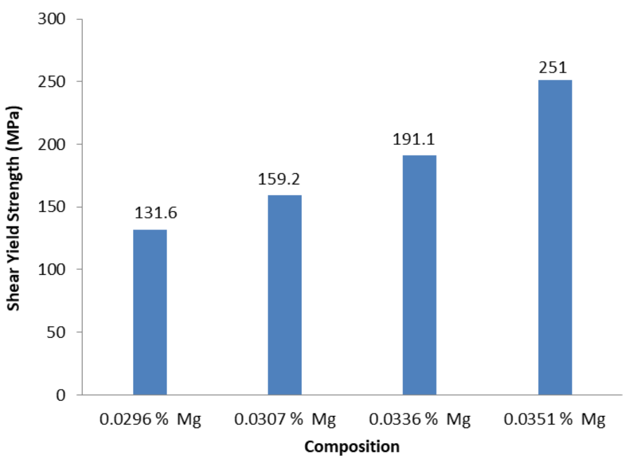

Figure 5: Effect magnesium composition on shear yield strength

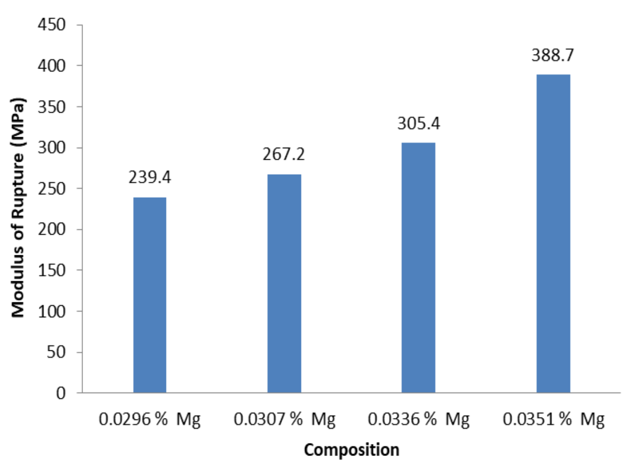

Figure 6: Effect magnesium composition on modulus of rupture

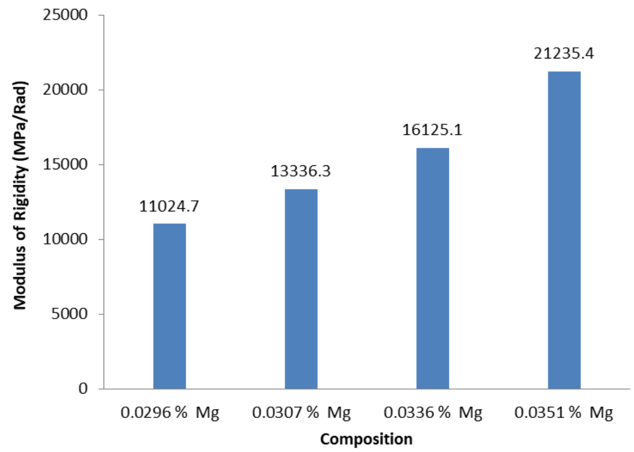

Figure 7: Effect magnesium composition on modulus of rigidity

4. CONCLUSION

Based on the results of the work, the following conclusions can be drawn:

The results of microstructure photographs on specimens with magnesium content of 0.0296%, 0.0307%, 0.0336%, and 0.0351% produce a black spheroidal graphite shape with a size tends to be smaller with the increasing percentage of the magnesium element composition contained in the nodular cast iron. The microstructure photograph also showed the increasing area of pearlite in the form of dark-coloured lamels and the reduction in the area of light-coloured ferrite around graphite in the nodular cast iron.

The results of the torsion test using the Torsee Testing Machine with ASTM E143 standard showed that increasing the magnesium content results in the increasing of strength (yield strength and modulus of rupture) as well as the increasing of stiffness (modulus of rigidity). This is due to an increase in the pearlite phase and reduced ferrite phase, where pearlite has a higher strength than ferrite and graphite.

Acknowledgement

The authors would like to acknowledge the mechanical engineering laboratory of Universitas Muhammadiyah Surakarta for facilitating the mechanical testing process.

REFERENCES

1. R. O. Giacomelli, D. B. Salvaro, C. Binder, A.N. Klein & J. D. B. de Mello (2018). **DLC deposited onto nitrided grey and nodular cast iron substrates: An unexpected tribological behaviour**. *Tribology International*, *121*, pp. 460-467. https://doi.org/10.1016/j.triboint.2018.02.009
2. K. Jhaveri, G.M. Lewis, J.L. Sullivan & G.A. Keoleian, (2018). **Life cycle assessment of thin-wall ductile cast**

iron for automotive lightweighting applications. *Sustainable Materials and Technologies*, *15*, pp. 1-8.

3. S. Schoenborn, H. Kaufmann, C.M. Sonsino & R. Heim (2016). **Variable amplitude fatigue of high-strength cast iron alloys for automotive applications**. *International Journal of Fatigue*, *91*, pp. 445-458. https://doi.org/10.1016/j.ijfatigue.2016.01.006
4. M. Pevec, G. Oder, I. Potrč, & M. Šraml (2014). **Elevated temperature low cycle fatigue of grey cast iron used for automotive brake discs**. *Engineering Failure Analysis*, *42*, pp. 221-230.
5. M.A. Bouaziz, M.A. Guidara, C. Schmitt, E. Hadj-Taïeb & Z. Azari (2014). **Water hammer effects on a gray cast iron water network after adding pumps**. *Engineering Failure Analysis*, *44*, pp. 1-16. https://doi.org/10.1016/j.engfailanal.2014.04.023
6. R. Jiang, S. Rathnayaka, B. Shannon, X.L. Zhao, J. Ji & J. Kodikara (2019). **Analysis of failure initiation in corroded cast iron pipes under cyclic loading due to formation of through-wall cracks**. *Engineering Failure Analysis*, *103*, pp. 238-248.
7. M. Gelfi, A. Pola, L. Girelli, A. Zacco, M. Masotti & G.M La Vecchia (2019). **Effect of heat treatment on microstructure and erosion resistance of white cast irons for slurry pumping applications**. *Wear*, *428*, pp. 438-448.
8. A. Sadeghi, A. Moloodi, M. Golestanipour & M. M. Shahri (2017). **An investigation of abrasive wear and corrosion behavior of surface repair of gray cast iron by SMAW**. *Journal of Materials Research and Technology*, *6*(1), pp. 90-95. https://doi.org/10.1016/j.jmrt.2016.09.003
9. I. C. Park & S.J. Kim (2019). **Effect of stabilizer concentration on the cavitation erosion resistance characteristics of the electroless nickel plated gray cast iron in seawater**. *Surface and Coatings Technology*, *376*, pp. 31-37.
10. I. Mitelea, I. Bordeaşu, M. Pelle & C. Crăciunescu (2015). **Ultrasonic cavitation erosion of nodular cast iron with ferrite–pearlite microstructure**. *Ultrasonics sonochemistry*, *23*, pp. 385-390.
11. T. N. F. Souza, R. A. P. S. Nogueira, F. J. S. Franco, M. T. P. Aguilar, & P.R. Cetlin (2014). **Mechanical and microstructural characterization of nodular cast iron (NCI) with niobium additions**. *Materials research*, *17*(5), pp. 1167-1172.
12. W. D. Callister & D. G. Rethwisch (2009). ***Materials science and engineering: an introduction,*** 8th ed. New York: Wiley.
13. A. de A Vicente, J. R. S. Moreno, T. F. de Abreu Santos, D. C. R. Espinosa & J. A. S. Tenório (2019). **Nucleation and growth of graphite particles in ductile cast iron**. *Journal of Alloys and Compounds*, *775*, pp. 1230-1234.
14. P. Čanžar, Z. Tonković & J. Kodvanj (2012). **Microstructure influence on fatigue behaviour of nodular cast iron**. *Materials Science and Engineering: A*, *556*, 88-99. https://doi.org/10.1016/j.msea.2012.06.062
15. O. O. Oluwole, O.E. Olorunniwo, O. O. Ogundare, P. O. Atanda & O.O. Oridota (2007). **Effect of magnesium and calcium as spheroidizer on the graphite morphology in ductile cast iron**. *Journal of Minerals & Materials Characterization & Engineering*, *6*(1), pp. 25-37.
16. M. Iasechko, V. Larin, D. Maksiuta, O. Ochkurenko, Ihor Krasnoshapka, Y. Samsonov, H. Lyashenko, A. Zinchenko & R. Vozniak (2019) **Model Description of the Modified Solid State Plasma Material for Electromagnetic Radiation Protection**, *International Journal of Emerging Trends in Engineering Research*, 7(10), 376-382. https://doi.org/10.30534/ijeter/2019/027102019
17. M. A. Habeeb & W.S. Mahdi (2019), **Characterization of (CMC-PVP- Fe2O3) Nanocomposites for Gamma Shielding Application**, *International Journal of Emerging Trends in Engineering Research*, 7(9), 247 - 255. https://doi.org/10.30534/ijeter/2019/06792019
18. E. Julianto, W.A. Siswanto & M. Effendy (2019), 7(9), **Characteristics of Temperature changes and Stress of Float Glass under Heat Radiation**, *International Journal of Emerging Trends in Engineering Research*, 7(9), 228 – 233 https://doi.org/10.30534/ijeter/2019/03792019
19. M. B. Karamış & K. Yıldızlı (2010). **Surface modification of nodular cast iron: A comparative study on graphite elimination**. *Materials Science and Engineering: A*, *527*(20), pp. 5225-5229.
20. B. Šamec, I. Potrč & M. Šraml (2011). **Low cycle fatigue of nodular cast iron used for railway brake discs**. *Engineering Failure Analysis*, *18*(6), pp. 1424-1434.
21. N. Li, S.M. Xing & P.W. Bao (2013). **Microstructure and mechanical properties of nodular cast iron produced by melted metal die forging process**. *Journal of Iron and Steel Research International*, *20*(6), pp. 58-62.
22. M. Benedetti, V. Fontanari & D. Lusuardi (2019). **Effect of graphite morphology on the fatigue and fracture resistance of ferritic ductile cast iron**, *Engineering Fracture Mechanics*, *206*, pp. 427-441.
23. A. Vaško, M. Uhríčik, L. Kuchariková & E. Tillová (2018). **Microstructure, mechanical and fatigue properties of SiMo-and SiCu-nodular cast irons**. *Procedia Structural Integrity*, *13*, pp. 1527-1532.
24. P. Kovacikova, R. Bezdedová & J. Vavro (2016). **Comparison of numerical analysis of stress-strain states of cast iron with vermicular graphite shape and globular graphite shape**. *Procedia Engineering*, *136*, pp. 28-32.

J. Khalil-Allafi & B. Amin-Ahmadi (2011). **Influence of mold preheating and silicon content on microstructure and casting properties of ductile iron in permanent mold**. *Journal of Iron and Steel Research International*, *18*(3), pp. 34-39.